

Strongly transverse-electric-polarized emission from deep ultraviolet AlGaIn quantum well light emitting diodes

Christoph Reich,^{1,a)} Martin Guttmann,¹ Martin Feneberg,² Tim Wernicke,¹ Frank Mehnke,¹ Christian Kuhn,¹ Jens Rass,^{1,3} Mickael Lapeyrade,³ Sven Einfeldt,³ Arne Knauer,³ Viola Kueller,³ Markus Weyers,³ Rüdiger Goldhahn,² and Michael Kneissl^{1,3}

¹Institut für Festkörperphysik, Technische Universität Berlin, Hardenbergstr. 36, Berlin 10623, Germany

²Institut für Experimentelle Physik, Otto-von-Guericke-Universität, Universitätsplatz 2, Magdeburg 39106, Germany

³Ferdinand-Braun-Institut, Leibniz-Institut für Höchstfrequenztechnik, Gustav-Kirchhoff-Str. 4, Berlin 12489, Germany

(Received 27 June 2015; accepted 27 September 2015; published online 5 October 2015)

The optical polarization of emission from ultraviolet (UV) light emitting diodes (LEDs) based on (0001)-oriented $\text{Al}_x\text{Ga}_{1-x}\text{N}$ multiple quantum wells (MQWs) has been studied by simulations and electroluminescence measurements. With increasing aluminum mole fraction in the quantum well x , the in-plane intensity of transverse-electric (TE) polarized light decreases relative to that of the transverse-magnetic polarized light, attributed to a reordering of the valence bands in $\text{Al}_x\text{Ga}_{1-x}\text{N}$. Using $\mathbf{k} \cdot \mathbf{p}$ theoretical model calculations, the AlGaIn MQW active region design has been optimized, yielding increased TE polarization and thus higher extraction efficiency for bottom-emitting LEDs in the deep UV spectral range. Using (i) narrow quantum wells, (ii) barriers with high aluminum mole fractions, and (iii) compressive growth on patterned aluminum nitride sapphire templates, strongly TE-polarized emission was observed at wavelengths as short as 239 nm. © 2015 AIP Publishing LLC. [<http://dx.doi.org/10.1063/1.4932651>]

Light emitting diodes (LEDs) in the deep ultraviolet (UVC) spectral region are of significant interest for applications in a variety of fields.^{1,2} However, the external quantum efficiency (EQE) of AlGaIn-based LEDs decreases rapidly when lowering the emission wavelength to values below 265 nm.³ Recently, we reported on the optimization of charge carrier injection,⁴ as well as improvement of the internal quantum efficiency (IQE) through growth on low-dislocation density AlN templates fabricated by epitaxial lateral overgrowth (ELO) of patterned AlN/sapphire.^{5,6} Additionally, the light extraction efficiency is also a challenge for UV emitters due to its strong dependence on the optical polarization of the emitted light. The emission pattern for transverse magnetic (TM, $\mathbf{E} \parallel \mathbf{c}$) polarized light is in-plane and thus the light extraction of TM-polarized light through the surface of a (0001) device is an order of magnitude smaller compared to transverse electric (TE, $\mathbf{E} \perp \mathbf{c}$) polarized light.⁷ In the $\text{Al}_x\text{Ga}_{1-x}\text{N}$ system, the topmost valence band splits into three energetically close subbands with different symmetry due to the spin-orbit and crystal field interaction. The radiative transition of an electron from the Γ_7 conduction band to a valence band is determined by the symmetry of the corresponding valence subband. The strong difference of the sign and the value of the crystal field energy between GaN (12.3 meV)⁸ and AlN (−221 meV)⁹ leads to switching of the valence band order and consequently to a change of the light polarization from TE polarization (GaN) to TM polarization (AlN) when pushing towards shorter emission wavelengths by increasing the aluminum mole fraction in the multiple quantum well (MQW).^{10–14} Therefore, the light extraction efficiency and thus the EQE

are dependent on the optical polarization and are significantly reduced for shorter wavelengths.

In this study, we report on the in-plane polarization dependence of LEDs emitting in the UVC spectral range. First, model calculations based on $\mathbf{k} \cdot \mathbf{p}$ -perturbation theory^{15,16} have been applied to investigate the light polarization for UVC LEDs with compressively strained quantum wells. Particularly, the dependence on the aluminum mole fraction in the quantum well x as well as in the barrier y were studied. Simulation results were subsequently used to design and fabricate UVC LEDs with an increased degree of TE polarization. Polarization-dependent electroluminescence (EL) measurements were then used to evaluate the light polarization properties.

Using model calculations based on $\mathbf{k} \cdot \mathbf{p}$ -perturbation theory, the dependence of light polarization and emission wavelengths on the quantum well design was studied. At first, a $\mathbf{k} \cdot \mathbf{p}$ -band model for strained wurtzite $\text{Al}_x\text{Ga}_{1-x}\text{N}$ layers was used to determine the conduction and valence band properties for the aluminum mole fractions x and y , e.g., band-edge energies, effective masses, and oscillator strengths as discussed by Chuang and Chang.¹⁶ Material parameters for GaN and AlN used in the calculations can be found in the literature.^{8,9,16–20} Band gap energies were calculated at room temperature ($T = 300\text{ K}$) using a bowing parameter $b = 0.9$ and assuming a linear change of the crystal field energy with the composition between the binary materials GaN and AlN.^{11,12} Using the equations for wurtzite semiconductors,¹⁶ the valence band order can be calculated. The topmost valence band in GaN is the heavy hole band with Γ_9 -symmetry, followed by the light hole band with Γ_{7+} -symmetry, and the split-off hole band with Γ_{7-} -symmetry. In contrast, in AlN, the topmost valence band has the

^{a)}Electronic mail: Christoph.Reich@tu-berlin.de

Γ_{7+} -symmetry, followed by Γ_9 and Γ_{7-} . As previously discussed, the optical polarization of a radiative recombination is determined by the symmetry of the corresponding valence band. Radiative recombination is predominantly comprised of holes from the top valence band (Γ_{7+}), and thus results in TM-polarized light emission for AlN, whereas in GaN, emission from radiative transitions to the topmost valence band (Γ_9) is strictly TE-polarized. In addition, the change of the valence band order involves an anti-crossing of the Γ_{7+} - and Γ_{7-} -bands, resulting in a change of oscillator strengths and polarization properties of the emission. This difference in the valence band order leads to a change of the light polarization from TE polarization (GaN) to TM polarization (AlN) with increasing aluminum mole fraction in the layer. The valence band-edge energies are strongly dependent on strain. In bulk-like $\text{Al}_x\text{Ga}_{1-x}\text{N}$ -layers, the calculated valence band crossing can be shifted from $x = 0.05$ for unstrained layers to $x = 0.55$ for compressively strained layers grown pseudomorphically on bulk AlN. Therefore, the switching of the light polarization shifts with increasing compressive biaxial strain towards higher aluminum mole fractions x .^{14,21} In addition to the dependence on the aluminum mole fraction x and the strain, the light polarization in quantum well structures is strongly influenced by the quantum confinement, due to different hole masses of the three valence bands.^{14,22} The quantum confinement is mainly determined by the barrier height as well as the well width.²³ With decreasing well width, the degree of polarization increases due to the increased influence of quantum confinement^{24,25} as well as due to the reduced quantum confined Stark effect (QCSE). In the simulations described in this paper, the quantum well width was kept constant at 1.5 nm. In our experience, quantum well widths <1.5 nm experimentally lead to poor injection efficiency and carrier leakage. Therefore, 1.5 nm was chosen as a compromise to achieve good performance and TE-polarized emission.

The quantum well band structure was calculated from the previously obtained conduction and valence band-edge energies of the well and the barrier. Following the conclusions of Northrup *et al.*,¹⁴ pseudomorphic growth on bulk AlN substrates was assumed, leading to compressively strained quantum wells. The model takes into account the QCSE, effective electron and hole masses of the three topmost valence bands, finite barrier heights, partial screening of electric fields by free carriers,¹⁴ and strain. Using a numerical matrix method to solve a discretized Schrödinger equation for the conduction band and the three topmost valence bands, the quantum well states and their wave functions were obtained.²⁶ For determining the degree of polarization, the overlap integrals of electron and hole wave functions as well as the interband momentum-matrix elements for TE- and TM-polarized emission were calculated¹⁶ assuming a Boltzmann-like thermal occupation of different valence bands and different quantum well states. The degree of in-plane light polarization ρ of a (0001) device is defined by

$$\rho = (I_{\text{TE}} - I_{\text{TM}})/(I_{\text{TE}} + I_{\text{TM}}),$$

where I_{TE} and I_{TM} are the integrated TE-polarized and TM-polarized light emission intensities, respectively.

Figure 1 shows simulation results of the degree of in-plane polarization at 300 K for quantum wells pseudomorphically grown on bulk AlN in dependence of the aluminum content in the quantum well x and the aluminum content in the barrier y . For a constant barrier height, a decrease of ρ with increasing aluminum content in the quantum well x can be observed. This fact can be explained by the decreasing distance between the Γ_9 - and the Γ_{7+} -band and the increased occupation of higher energy states. At higher aluminum mole fractions x , the reordering of the two topmost valence bands as well as change of the interband momentum-matrix elements leads to a switching of the light polarization (dotted line) from TE to TM.

Furthermore, for constant x in the quantum well, the degree of polarization ρ increases with increasing aluminum content in the barrier y , becoming more TE-polarized. Thus, the limit for LEDs with dominant TE-polarized emission can be pushed towards even shorter emission wavelengths by using barriers with high aluminum mole fractions. The strong increase of TE polarization with increasing barrier height can be explained by the higher effective mass of the heavy hole valence band (Γ_9 -band), yielding TE polarization compared to the light hole valence band (Γ_{7+} -band). Thus, the degree of light polarization shifts towards TE with increasing barrier height. In a previous study of LEDs grown on relaxed AlGaIn templates, Kolbe *et al.* experimentally determined the TE/TM switching to be at 300 nm,¹³ whereas our simulations indicate the TE/TM switching at shorter wavelengths. This difference can be attributed to higher compressive strain in quantum wells grown pseudomorphically on AlN.

Highly compressively strained quantum wells due to pseudomorphic growth on AlN bulk are beneficial for achieving TE-polarized emission. An alternative to AlN bulk substrates is the use of AlN templates fabricated by ELO⁵ of patterned AlN/sapphire. The ELO/AlN-layers even exhibit a slightly increased amount of compressive in-plane strain ($\epsilon_{xx} = 0.002$) due to differences of thermal expansion coefficients and the coalescence process. Similar model calculations for quantum wells strained to ELO/AlN have been

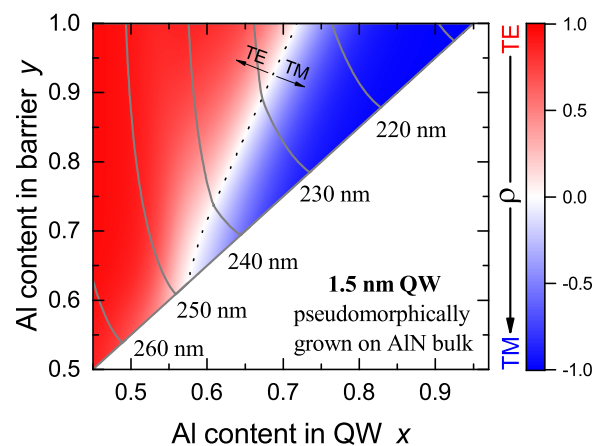


FIG. 1. Degree of polarization ρ of the emission from AlGaIn-based quantum wells pseudomorphically grown on AlN bulk, obtained by $\mathbf{k} \cdot \mathbf{p}$ -perturbation theory. The polarization switching (dotted line) shifts towards shorter wavelengths when increasing the barrier height (vertical axis). The gray lines indicate compositions with constant emission wavelengths.

performed and are shown in Figure 2. With this increased compressive strain, the switching of the light polarization is affected, and shifts by 8 nm towards shorter emission wavelengths compared to quantum wells grown on AlN bulk. Therefore, the ELO approach enables the realization of predominantly TE-polarized light emitters in the deep UV spectral range, outperforming heterostructures grown on relaxed AlGaN/sapphire or even homoepitaxial AlN. Summarizing our simulations, it is possible to obtain strongly TE-polarized light from UVC LEDs when using compressively strained MQWs and quantum barriers with high aluminum mole fractions.

These quantitatively obtained design rules for LEDs with increased TE polarization were tested experimentally. The UVC LEDs were grown by metalorganic vapor phase epitaxy using standard precursors (NH_3 , TMAI, TMGa, TEGa) and dopant sources (SiH_4 and Cp_2Mg) on low dislocation density (0001) ELO AlN/sapphire templates.⁵ The heterostructures consist of a highly conductive AlGaN:Si current spreading layer,²⁷ a threefold $\text{Al}_x\text{Ga}_{1-x}\text{N}/\text{Al}_y\text{Ga}_{1-y}\text{N}$ MQW active region, and a p-AlGaN electron blocking heterostructure.⁴ The emission wavelength was varied by changing the aluminum content in the quantum well x . The aluminum content y in the barrier was also adjusted so that the high energy offset between quantum well and barrier remained constant for all LED samples. The composition range used for the fabricated UVC LEDs is indicated by dotted yellow lines in Figure 2. The LEDs were processed with standard chip-processing technologies. Inductively coupled plasma etching was used to fabricate $100\ \mu\text{m} \times 100\ \mu\text{m}$ mesa structures by etching down to the n-AlGaN exposing the active region of the LED at the mesa sidewall. Palladium-based p-contacts and Vanadium-based n-contacts were deposited to form the electrodes.²⁸ The mesa sidewalls are not passivated to enable in-plane light emission in the polarization-dependent EL measurements. High resolution X-ray diffraction measurements confirmed pseudomorphic (compressive) growth of the LED heterostructure on the ELO/AlN ($a = 3.1057\ \text{\AA}$). The influence of small strain fluctuations due to the $3\ \mu\text{m}$ -period stripe pattern⁵ of the ELO can be neglected due to the larger p-contact size

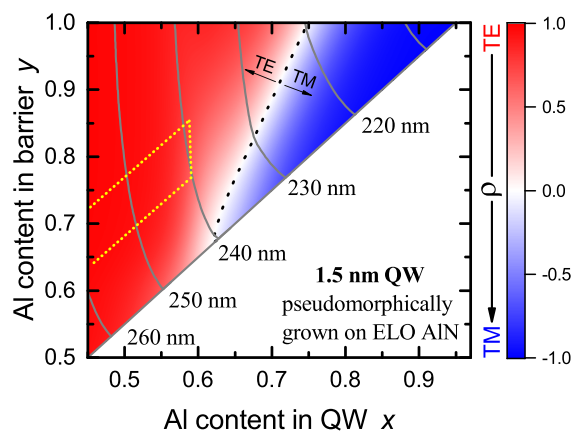


FIG. 2. Degree of polarization ρ of quantum well structures pseudomorphically grown on ELO AlN/sapphire, obtained by $\mathbf{k} \cdot \mathbf{p}$ -perturbation theory. In comparison to structures grown on bulk AlN, the polarization switching occurs at higher aluminum content x in the quantum well (horizontal axis) and thus at shorter emission wavelengths. The dotted yellow lines indicate the composition range used for the UVC LEDs fabricated in this study.

($100\ \mu\text{m} \times 100\ \mu\text{m}$). Measurements of the spectra, the optical power, and the polarization degree were performed at continuous drive current of either 20 mA in bottom-emitter configuration or 5 mA for in-plane emission from the mesa sidewall. The low current density of $50\ \text{A}/\text{cm}^2$ for in-plane emission prevents heating of the LED devices during polarization-dependent EL measurements. The in-plane emission was analyzed by a polarization-dependent EL setup using a Glan-Taylor-prism. The detailed description of the setup can be found elsewhere.¹³

The spectra of five UVC LEDs with different composition of the quantum well, corresponding to decreasing emission wavelengths from 263 nm to 239 nm, are shown in Figure 3. The total output power decreases rapidly with decreasing wavelengths. This fact is mainly due to the drop of carrier injection efficiency at shorter wavelengths.⁴ However, a decrease of the TE-polarized part of the emission could lead to a reduction of the light extraction efficiency. The absolute intensities shown in Figure 3 may also be influenced by different nonradiative recombination rates of the different samples. Nevertheless, the polarization properties are expected to be defined by the population of the subbands and therefore are independent of different nonradiative recombination rates. Figure 4 shows the polarization-dependent in-plane emission spectra of the five LEDs previously shown in Fig. 3. All spectra are normalized to the maximum of the TE-polarized spectrum. As expected, the fraction of the TM-polarized emission increases when decreasing the wavelength. However, the TE polarization is dominant in all LEDs, even down to emission wavelengths of 239 nm, which is consistent with our simulations.

The degree of in-plane polarization ρ is calculated from the integrated intensity of these spectra, and is shown in Figure 5. Between 265 nm and 250 nm, the polarization degree is almost constant at $\approx +0.8$. The maximum ρ is limited by the collection of unpolarized stray light. Below 250 nm, the degree of in-plane polarization decreases with decreasing wavelength. However, even at 239 nm, the polarization ratio is still around $+0.5$. The observed trend of the polarization degree confirms the predictions (green stars in

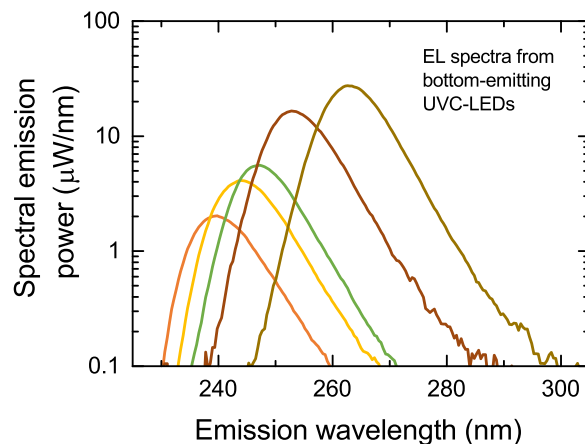


FIG. 3. Electroluminescence emission spectra of selected UVC LEDs measured at room temperature ($T = 300\ \text{K}$). $100\ \mu\text{m} \times 100\ \mu\text{m}$ -contacts were used at a continuous drive current of 20 mA in bottom-emitter configuration.

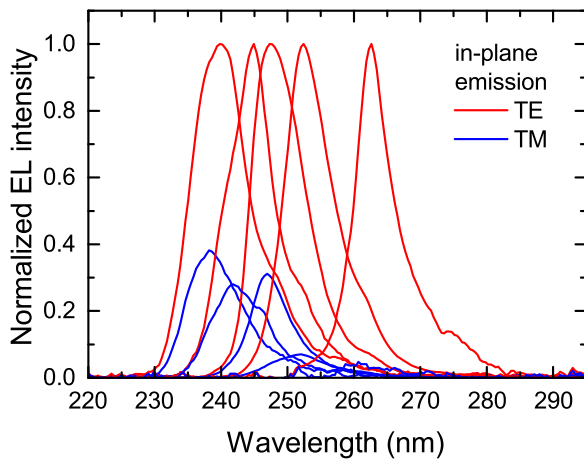


FIG. 4. Polarization-dependent in-plane emission spectra of selected UVC LEDs. The devices were operated at continuous drive current of 5 mA at room temperature ($T = 300$ K). All EL spectra are normalized to the maximum TE-polarized intensity. The spectra taken for the TE and TM polarization are shown in red and blue colors, respectively.

Fig. 5) obtained from our simulations. This decrease partly explains the stronger decrease of the EL intensity below 250 nm in bottom-emitter configuration (Fig. 3), suggesting slightly increased influence of the light polarization on the external quantum efficiency for shorter emission wavelengths. The light extraction efficiency is currently under investigation using ray-tracing simulations. Preliminary results suggest that an increase of the degree of polarization from TM ($\rho = -1$) to $\rho = +0.5$ at 239 nm could lead to an increase of the light extraction by a factor of 2–3 in agreement to Ryu *et al.*⁷ In comparison to previous results for UVA and UVB LEDs, where a TE/TM polarization switching was observed at 300 nm,¹³ we observe dominant TE polarization at much shorter wavelengths. This fact can be explained to some extent by the shift of the valence band crossing towards higher aluminum mole fractions with increasing compressive in-plane strain. In addition, high barriers and narrow quantum wells in our UVC LED design

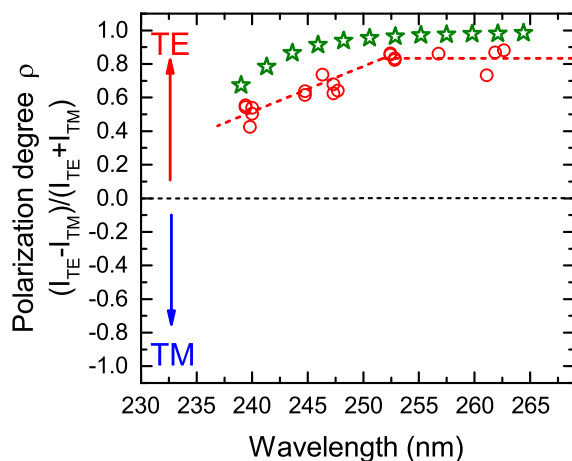


FIG. 5. Experimentally obtained degree of polarization ρ (circles) from in-plane EL measurements on LEDs with different emission wavelengths operated at continuous drive current of 5 mA at room temperature. All LEDs show strong TE polarization. The red dashed line is a guide-to-the-eye. As a comparison, values of ρ obtained from simulations are included as green stars.

result in a larger quantum confinement, favoring TE-polarized emission in the deep UV spectral range.

In conclusion, we studied the influence of design parameters for the active region of UVC LEDs on the polarization of the emitted light, using model calculations based on $\mathbf{k} \cdot \mathbf{p}$ perturbation theory. Compressive strain in the growth-plane and high quantum barriers are beneficial for enhanced TE-polarized emission, even at short wavelengths in the UVC spectral range. Strongly TE-polarized light emission was obtained from multiple quantum well UVC LEDs pseudo-morphically grown on compressively strained ELO AlN/sapphire templates.

This work has been funded by the German Research Foundation within the Collaborative Research Center 787 “Semiconductor Nanophotonics” and by the German Federal Ministry of Education and Research within the “UltraSens” Project (Nos. 13N12587 and 13N12588). The authors thank Benjamin Neuschl and Ingrid Koslow for fruitful discussions.

¹M. Würtele, T. Kolbe, M. Lipsz, A. Külberg, M. Weyers, M. Kneissl, and M. Jekel, *Water Res.* **45**, 1481 (2011).

²R. J. Drost and B. M. Sadler, *Semicond. Sci. Technol.* **29**, 084006 (2014).

³M. Kneissl, T. Kolbe, C. Chua, V. Kueller, N. Lobo, J. Stellmach, A. Knauer, H. Rodriguez, S. Einfeldt, Z. Yang, N. M. Johnson, and M. Weyers, *Semicond. Sci. Technol.* **26**, 014036 (2011).

⁴F. Mehnke, C. Kuhn, M. Guttman, C. Reich, T. Kolbe, V. Kueller, A. Knauer, M. Lapeyrade, S. Einfeldt, J. Rass, T. Wernicke, M. Weyers, and M. Kneissl, *Appl. Phys. Lett.* **105**, 051113 (2014).

⁵V. Kueller, A. Knauer, C. Reich, A. Mogilatenko, M. Weyers, J. Stellmach, T. Wernicke, M. Kneissl, Z. Yang, C. Chua, and N. Johnson, *IEEE Photonics Technol. Lett.* **24**, 1603 (2012).

⁶C. Reich, M. Feneberg, V. Kueller, A. Knauer, T. Wernicke, J. Schlegel, M. Frentrup, R. Goldhahn, M. Weyers, and M. Kneissl, *Appl. Phys. Lett.* **103**, 212108 (2013).

⁷H.-Y. Ryu, I.-G. Choi, H.-S. Choi, and J.-I. Shim, *Appl. Phys. Express* **6**, 062101 (2013).

⁸R. Ishii, A. Kaneta, M. Funato, Y. Kawakami, and A. A. Yamaguchi, *Phys. Rev. B* **81**, 155202 (2010).

⁹M. Feneberg, M. F. Romero, M. Röppischer, C. Cobet, N. Esser, B. Neuschl, K. Thonke, M. Bickermann, and R. Goldhahn, *Phys. Rev. B* **87**, 235209 (2013).

¹⁰K. B. Nam, J. Li, M. L. Nakarmi, J. Y. Lin, and H. X. Jiang, *Appl. Phys. Lett.* **84**, 5264 (2004).

¹¹B. Neuschl, J. Helbing, M. Knab, H. Lauer, M. Madel, K. Thonke, T. Meisch, K. Forghani, F. Scholz, and M. Feneberg, *J. Appl. Phys.* **116**, 113506 (2014).

¹²M. Feneberg, M. Winkler, J. Klamser, J. Stellmach, M. Frentrup, S. Ploch, F. Mehnke, T. Wernicke, M. Kneissl, and R. Goldhahn, *Appl. Phys. Lett.* **106**, 182102 (2015).

¹³T. Kolbe, A. Knauer, C. Chua, Z. Yang, S. Einfeldt, P. Vogt, N. M. Johnson, M. Weyers, and M. Kneissl, *Appl. Phys. Lett.* **97**, 171105 (2010).

¹⁴J. Northrup, C. Chua, Z. Yang, T. Wunderer, M. Kneissl, N. Johnson, and T. Kolbe, *Appl. Phys. Lett.* **100**, 021101 (2012).

¹⁵M. Feneberg, F. Lipski, R. Sauer, K. Thonke, P. Bruckner, B. Neubert, T. Wunderer, and F. Scholz, *J. Appl. Phys.* **101**, 053530 (2007).

¹⁶S. Chuang and C. Chang, *Phys. Rev. B* **54**, 2491 (1996).

¹⁷R. Ishii, A. Kaneta, M. Funato, and Y. Kawakami, *Phys. Rev. B* **87**, 235201 (2013).

¹⁸M. Feneberg, K. Lange, C. Lidig, M. Wieneke, H. Witte, J. Blsing, A. Dadgar, A. Krost, and R. Goldhahn, *Appl. Phys. Lett.* **103**, 232104 (2013).

¹⁹A. Polian, M. Grimsditch, and I. Grzegory, *J. Appl. Phys.* **79**, 3343 (1996).

²⁰M. Kazan, E. Moussaed, R. Nader, and P. Masri, *Phys. Status Solidi C* **4**, 204 (2007).

²¹M. Funato, K. Matsuda, R. G. Banal, R. Ishii, and Y. Kawakami, *Phys. Rev. B* **87**, 041306 (2013).

- ²²R. G. Banal, M. Funato, and Y. Kawakami, *Phys. Rev. B* **79**, 121308 (2009).
- ²³J. J. Wierer, I. Montañó, M. H. Crawford, and A. A. Allerman, *J. Appl. Phys.* **115**, 174501 (2014).
- ²⁴T. M. Al Tahtamouni, J. Y. Lin, and H. X. Jiang, *Appl. Phys. Lett.* **101**, 042103 (2012).
- ²⁵T. Sharma, D. Naveh, and E. Towe, *Phys. Rev. B* **84**, 035305 (2011).
- ²⁶J. F. Van der Maelen Uría, S. García-Granda, and A. Menéndez-Velázquez, *Am. J. Phys.* **64**, 327 (1996).
- ²⁷F. Mehnke, T. Wernicke, H. Pingel, C. Kuhn, C. Reich, V. Kueller, A. Knauer, M. Lapeyrade, M. Weyers, and M. Kneissl, *Appl. Phys. Lett.* **103**, 212109 (2013).
- ²⁸M. Lapeyrade, A. Muhin, S. Einfeldt, U. Zeimer, A. Mogilatenko, M. Weyers, and M. Kneissl, *Semicond. Sci. Technol.* **28**, 125015 (2013).